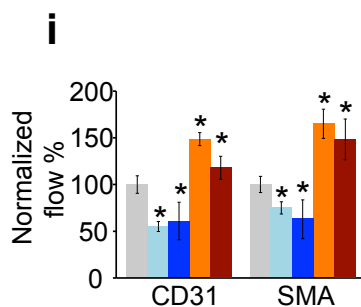
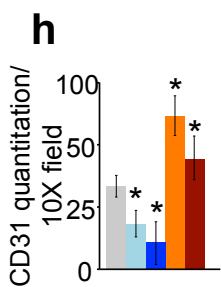
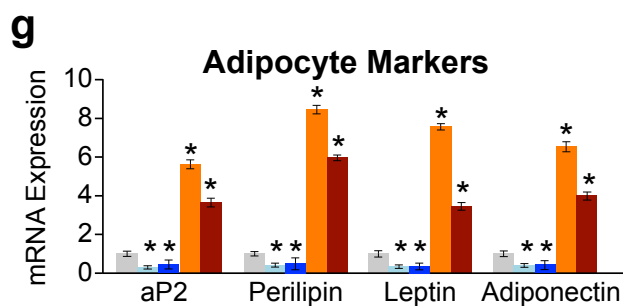
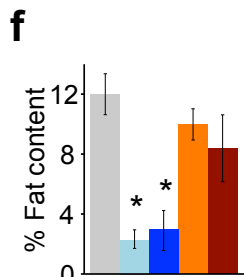
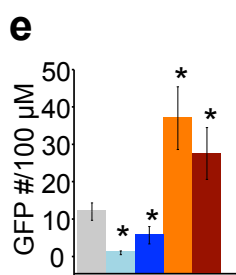
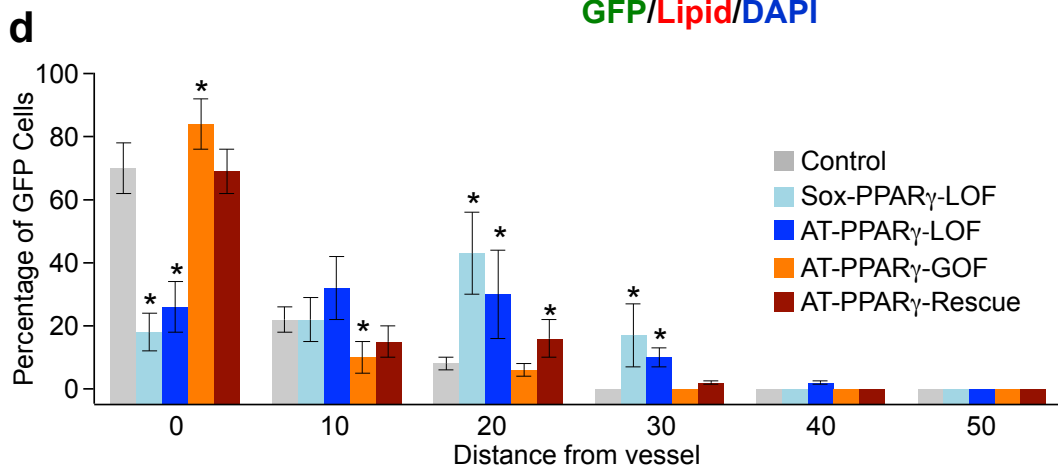
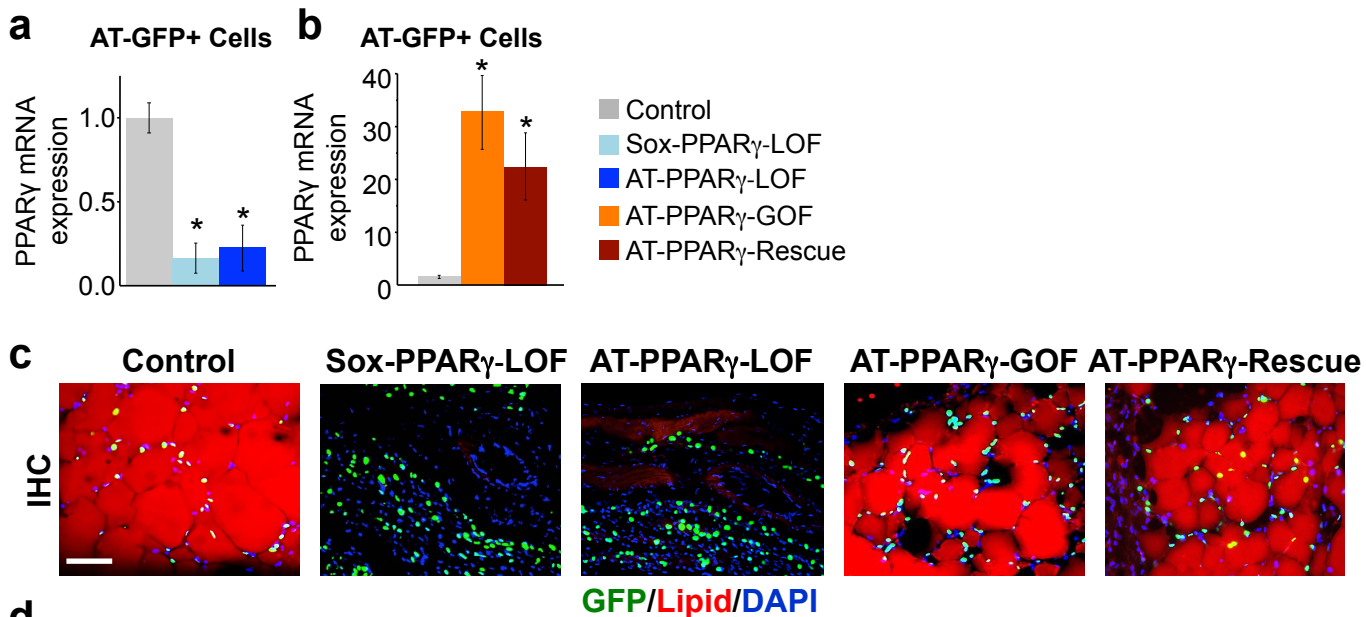


Title of file for HTML: Peer Review File

Description:

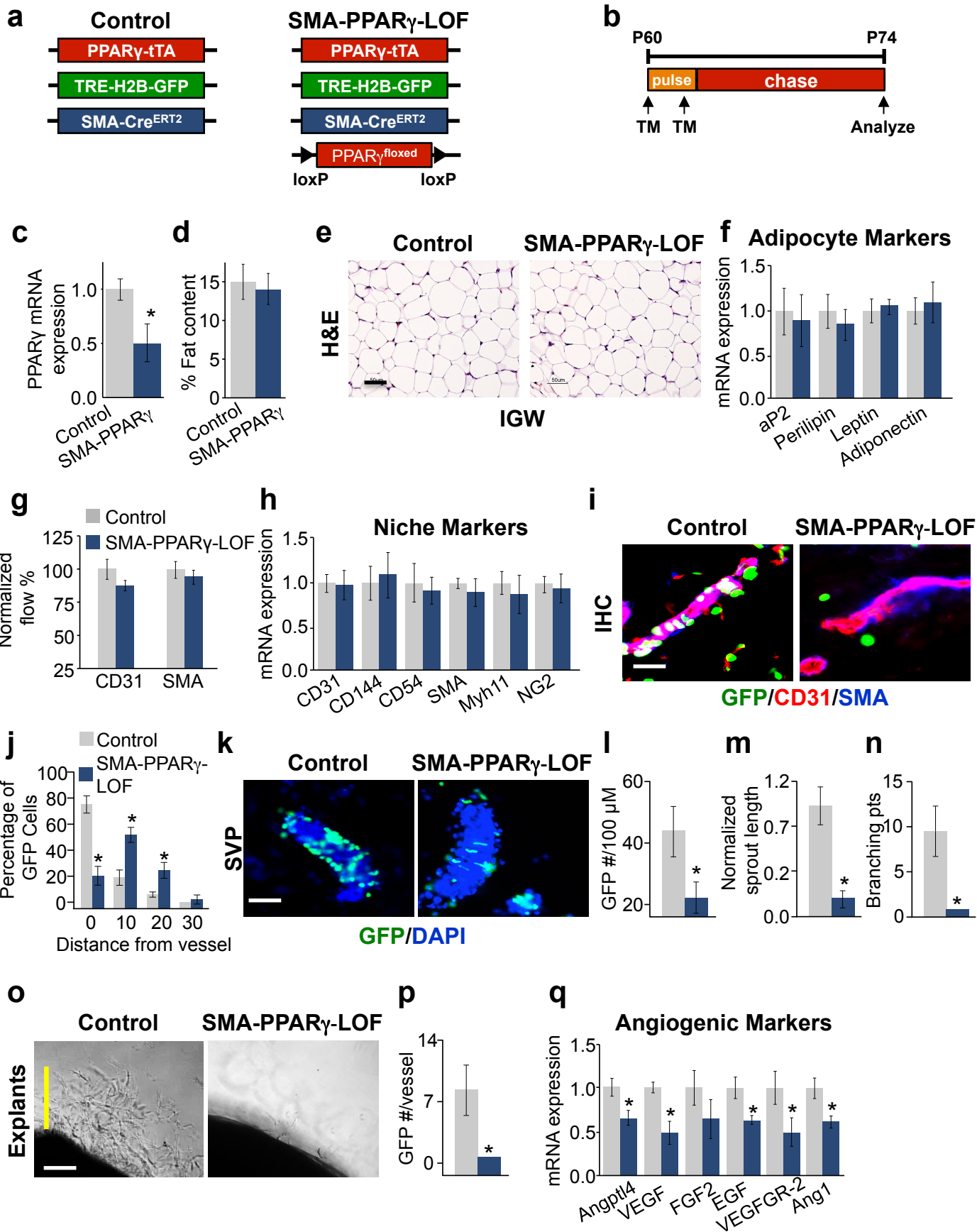
Title of file for HTML: Supplementary Information

Description: Supplementary Figures and Table.



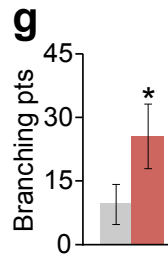
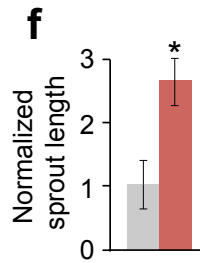
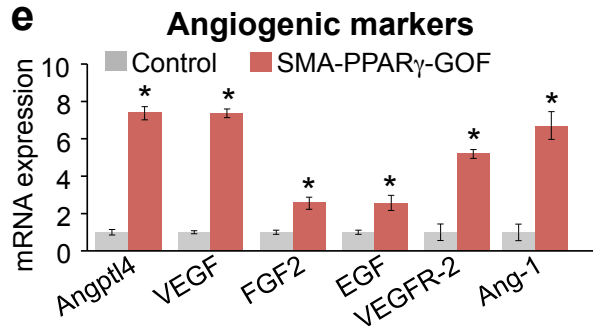
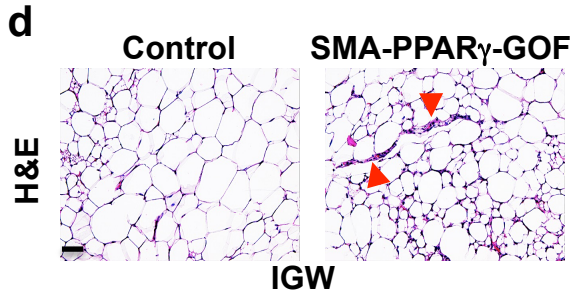
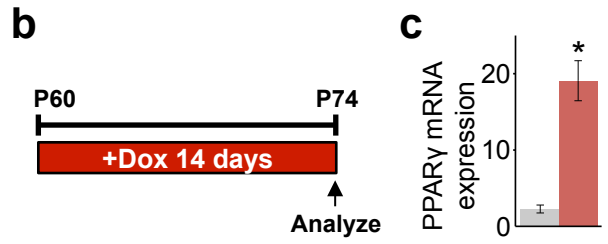
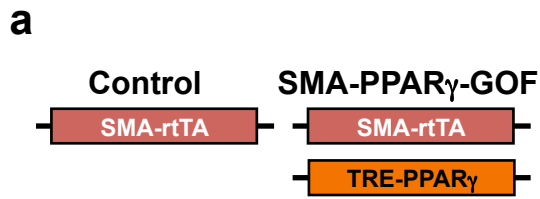
Supplementary Fig. 1 PPAR γ is not required for adipose depot developmental patterning

(a,b) AT-GFP⁺ cells were FACS isolated from AdipoTrak control (PPAR γ^{tTA} ; TRE-H2B-GFP), Sox-PPAR γ -LOF (Sox2-Cre; PPAR $\gamma^{f/tTA}$; TRE-H2B-GFP), AT-PPAR γ -LOF (TRE-Cre; PPAR $\gamma^{f/tTA}$; TRE-H2B-GFP), AT-PPAR γ -GOF (PPAR γ^{tTA} ; TRE-PPAR γ ; TRE-H2B-GFP) and AT-PPAR γ -Rescue (TRE-Cre; PPAR $\gamma^{f/tTA}$; TRE-PPAR γ ; TRE-H2B-GFP) and mRNA expression of PPAR γ was examined. Experiments were performed three times on 6 mice/group. (c) Representative images of lipid (LipidTox) stained cyrosections from subcutaneous IGW depots from the GFP labeled mice described in (a). DAPI was used to visual nuclei and cell number. Scale Bar 100 μ m. (d) Quantification of AT-GFP distance away from CD31/SMA⁺ blood vessels from sections described in Figure 1d. (e) Representative images of SVPs isolated from mice described in (a). AT-GFP number was quantified per 100-micron SVP. (f) Fat content from mice described in (a). (g) Quantitative RT-PCR analysis of adipocyte markers from mice described in (a). (h) Number of CD31⁺ cells were quantified from immunostained sections from subcutaneous IGW depots from denoted mice. (i) The SV compartment was isolated from mice described (a). Cells were stained with antibodies against CD31 and SMA and analyzed by flow cytometry. * $P < 0.05$ unpaired t-test, two-tailed: mutants compared to control. Data are expressed as means \pm s.em.



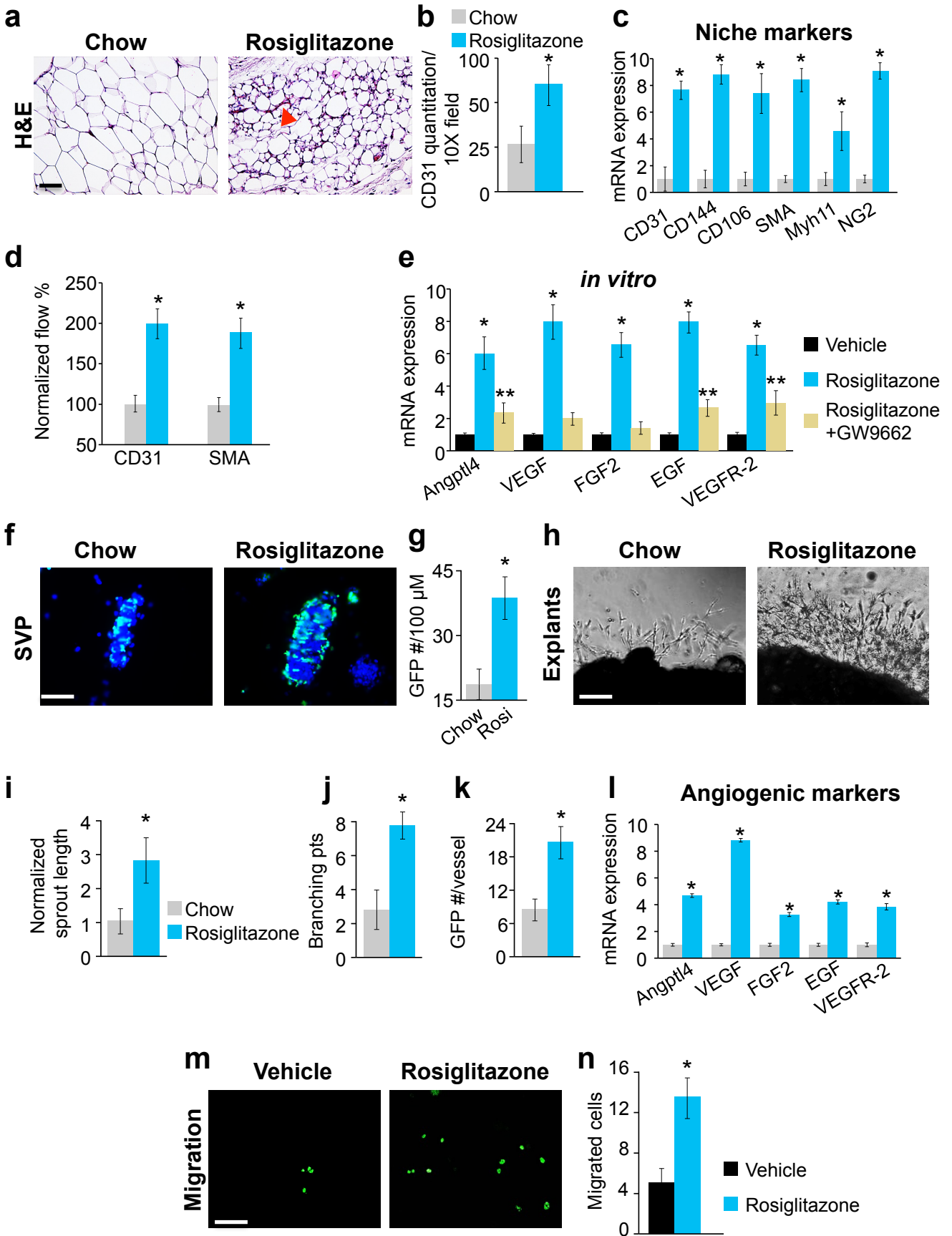
Supplementary Fig. 2 Adult APC PPAR γ expression is required for WAT niche expansion and APC-niche interaction

(a) Illustration of genetic alleles used to generate: AdipoTrak-SMA control (PPAR $\gamma^{+/fTA}$; TRE-H2B-GFP; SMA-Cre^{ERT2}) and SMA-PPAR γ -LOF (SMA-Cre^{ERT2}; PPAR $\gamma^{f/fTA}$; TRE-H2B-GFP). (b) Diagram of experimental paradigm. Mice were administered one dose of tamoxifen (50 mg/ Kg) for two consecutive days. Mice were then chased for 14 days. Experiments were performed three times on 10 mice/group. (c) Quantitative RT-PCR analysis of PPAR γ mRNA expression from SV cells after the 14 day chase. (d) Fat content of mice described in (a). (e) Representative images of H&E staining of subcutaneous IGW depots from mice described in (a). Scale Bar 50 μ m. (f) Quantitative RT-PCR analysis of adipocyte markers from whole adipose tissue from mice described in (a). (g) The SV compartment was isolated from mice described (a). Cells were stained with antibodies against CD31 and SMA and were analyzed by flow cytometry for expression. (h) Quantitative RT-PCR analysis of niche markers (endothelial and mural cell markers) from the SV compartment of adipose depots from mice described in (a). (i) Representative images of CD31 (endothelial), SMA (mural) and AT-GFP staining of subcutaneous IGW depots from mice described in (a). (j) Quantification of AT-GFP distance away from CD31/SMA⁺ blood vessels from sections described in (i). (k) Representative images of SVPs isolated from subcutaneous adipose depots from mice described in (a). AT-GFP locality was assessed and DAPI was used to visual nuclei. Scale Bar 100 μ m. (l) Quantification of AT-GFP APC occupancy per 100 micron of SVPs. (m-p) Representative images of vascular sprouts from subcutaneous IGW depots from the mice described in (a). Sprout length (m), branching (n), sprouting (o), and AT-GFP sprout occupancy (p) were quantified. * $P < 0.01$ unpaired t-test, two-tailed: mutant compared to control. Data are expressed as means \pm s.e.m.



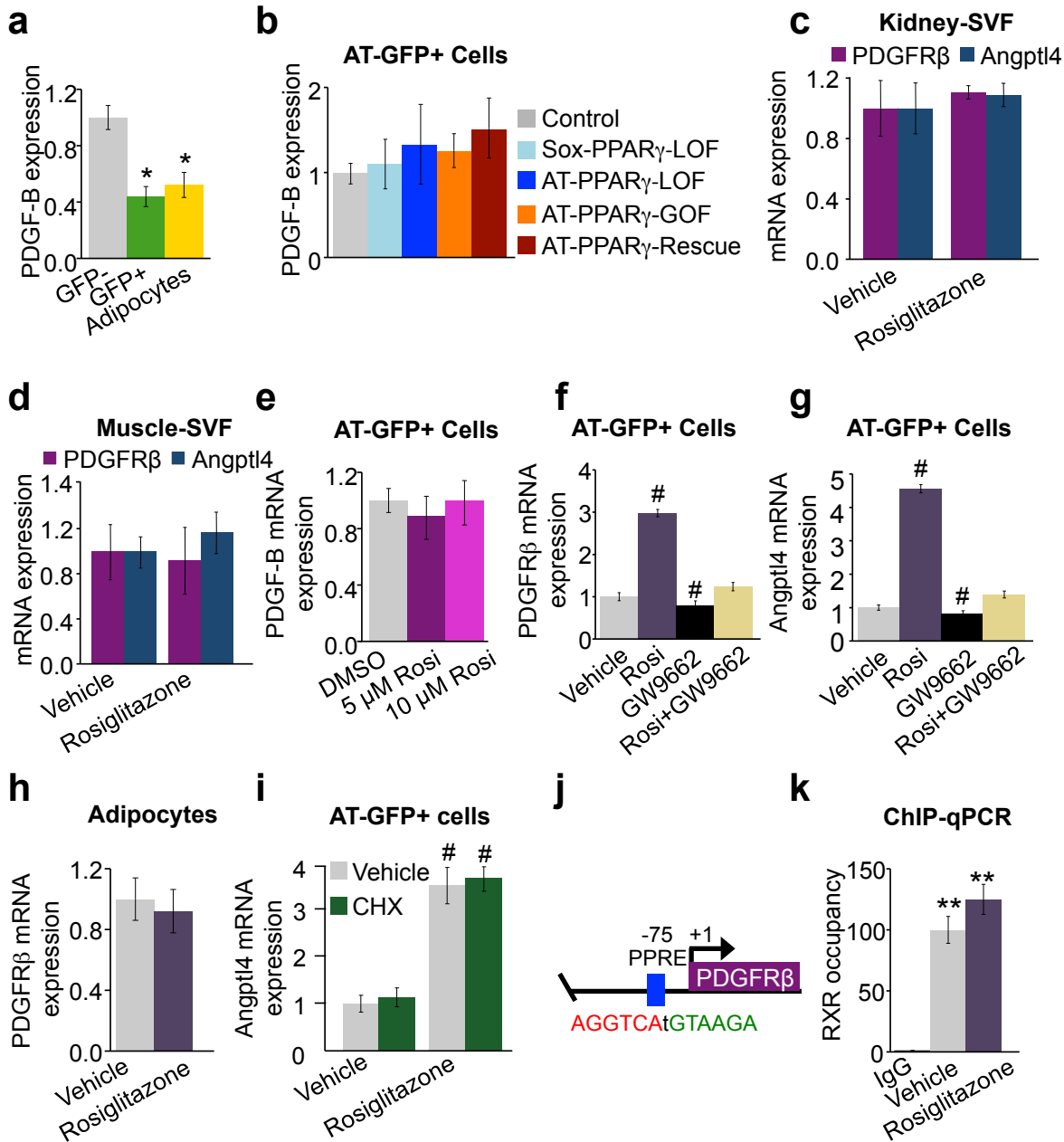
Supplementary Fig. 3 Adult APC PPAR γ expression is required for WAT niche expansion and APC-niche interaction

(a) Illustration of genetic alleles used to generate: control (SMA-rtTA) and SMA-PPAR γ -GOF (SMA-rtTA; TRE-PPAR γ). (b) Diagram of experimental paradigm; mice were administered doxycycline (0.5 mg/ Kg) for 14 consecutive days. Experiments were performed three times on 8 mice/group. (c) Quantitative RT-PCR analysis of PPAR γ mRNA expression from SV cells after the 14 day chase. (d) Representative images of H&E staining of subcutaneous IGW depots from mice described in (a). Red arrowheads indicate adipose tissue vasculature. Scale Bar 100 μ m. (e) Quantitative RT-PCR analysis of angiogenic markers of SV cells from mice described in (a). (f,g) Vascular sprout length (f) and branching (g) were quantified from subcutaneous IGW depots from the mice described in (a) * P <0.05 unpaired t-test, two-tailed: mutant compared to control. Data are expressed as means \pm s.e.m.



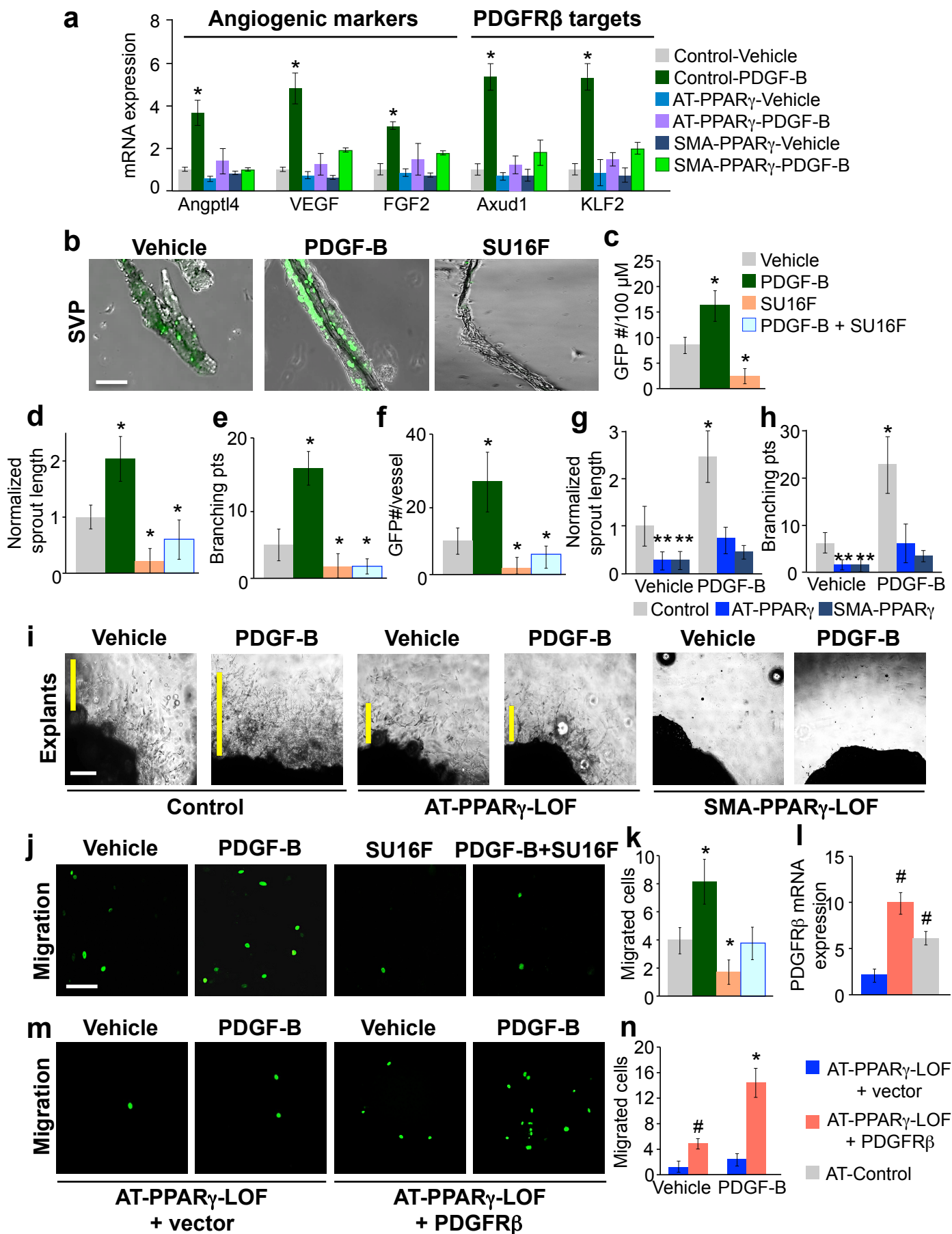
Supplementary Fig. 4 TZD's stimulate WAT niche expansion and APC-niche interaction

(a) AdipoTrak control mice were administered normal chow or rosiglitazone supplemented chow (0.0075% diet) for 2 weeks and then analyzed for nichegenic potential and progenitor cell dynamics. Experiments were performed three times on 10 mice/group. Representative images of H&E staining of subcutaneous IGW depot. Red arrowhead indicates adipose tissue vasculature. Scale Bar 100 μ m. (b) Number of CD31+ cells were quantified from immunostained sections from subcutaneous IGW depots from chow and rosiglitazone treated mice as described in (a). (c) Quantitative RT-PCR analysis of endothelial and mural cell markers from SV cells from mice described in (a). (d) Total SV cells were isolated from mice described in (a) and were stained with antibodies against CD31 and SMA. Positive cells were quantified by flow cytometry. (e) Total SV cells were pre-treated with vehicle or GW9662 (5 μ M), a PPAR γ antagonist for 15 mins, subsequently cells were treated with vehicle or rosiglitazone (1 μ M) for 12 hours. Angiogenic gene expression was monitored. (f,g) Representative images of SVPs isolated from subcutaneous IGW depots from mice described in (a). SVPs were not supplemented with rosiglitazone *ex-vivo*. AT-GFP locality was assessed 12 hours after isolation (f). AT-GFP number were quantified per 100 micron SVP (g). Scale Bar 100 μ m. (h-k) Representative images of vascular explants from subcutaneous IGW depots from mice described in (a). Vascular sprout length (i), branching points (j) and GFP progenitor occupancy (k) were quantified. Scale Bar 100 μ m. (l) Quantitative RT-PCR analysis of angiogenic markers from subcutaneous IGW depots from mice described in (a). (m,n) SV cells were isolated from the mice described in (a) and AT-GFP+ were FACS isolated. Cells were cultured in modified Boyden transwell chambers. Cells were continually cultured with vehicle (DMSO) or rosiglitazone (1 μ M). Migration was assessed 12 hours later (m) and AT-GFP number was quantified (n). Scale Bar 100 μ m. * P <0.05 unpaired t-test, two-tailed: rosiglitazone treated compared to vehicle treated. ** P <0.05 unpaired t-test, two-tailed: GW9662 + rosiglitazone compared to rosiglitazone alone. Data are expressed as means \pm s.e.m.



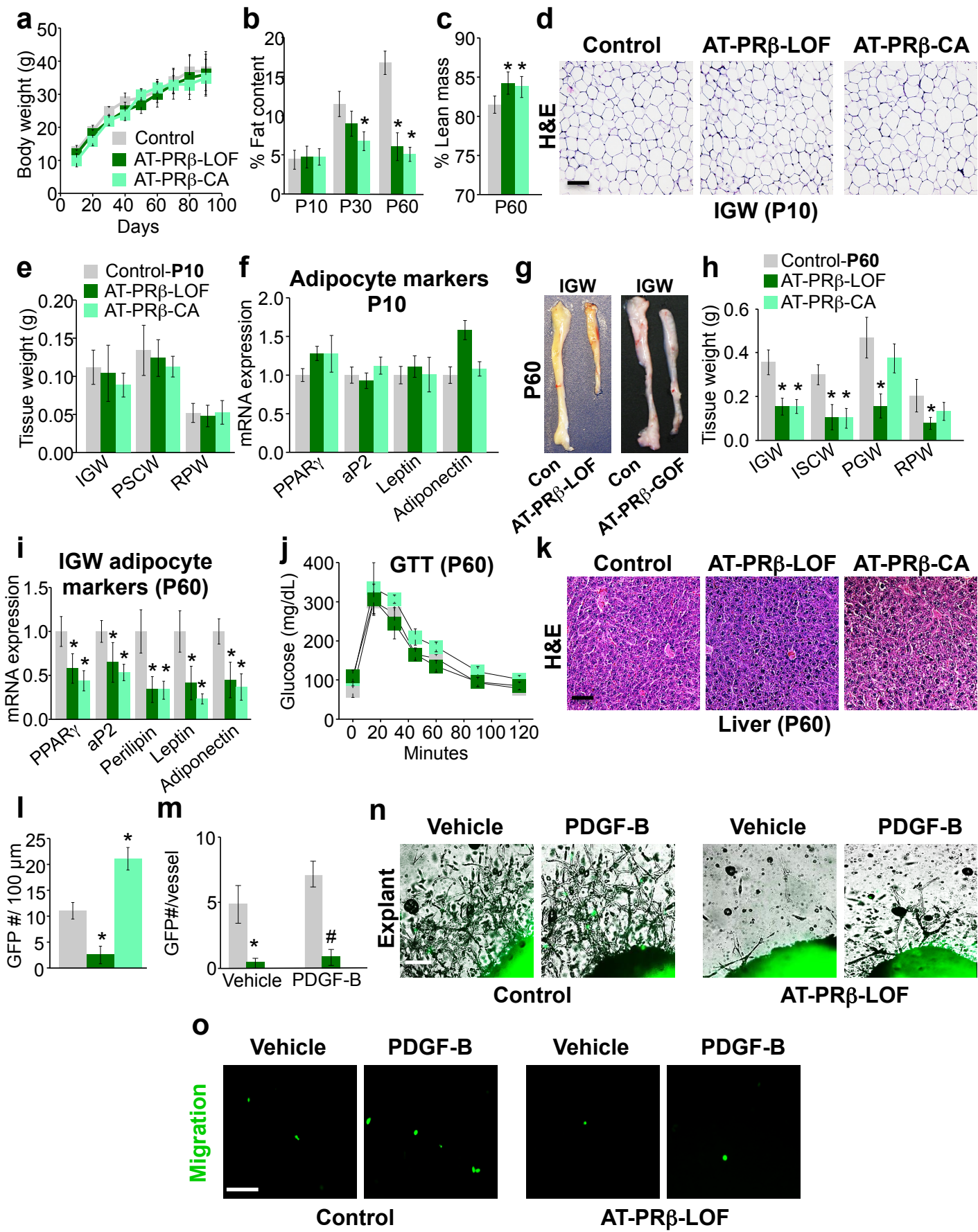
Supplementary Fig. 5 PPAR γ transcriptionally controls niche formation, expansion and APC-niche interaction

(a) GFP⁻ and AT-GFP⁺ cells were FACS isolated from AT-control mice ($n = 6$) and adipocytes were isolated by floatation. PDGF-B mRNA expression was measured. * $P < 0.01$ compared to SV GFP negative cells. (b) AT-control, Sox-PPAR γ -LOF, AT-PPAR γ -LOF, AT-PPAR γ -GOF and AT-PPAR γ -Rescue were administered normal chow or rosiglitazone chow (0.0075%) for 7 days ($n = 10$). Subsequently, AT-GFP⁺ cells were FACS isolated and PDGF-B mRNA expression was measured. (c,d) Quantitative RT-PCR analysis of PDGFR β and Angptl4 mRNA from SV cells isolated from kidney (c) and muscle (d) from mice described in (b). (e) GFP⁺ cells were FACS isolated from AT-GFP control mice ($n = 6$) and treated with denoted concentrations of rosiglitazone for 4 hours. mRNA expression of PDGF-B was measured. (f,g) Quantitative RT-PCR analysis of PDGFR β and Angptl4 mRNA from FACS isolated AT-GFP⁺ from AT-control mice ($n = 6$) pre-treated with vehicle (DMSO) or GW9662 (5 μ M) and then treated with vehicle (DMSO) or rosiglitazone (1 μ M). # $P < 0.05$ unpaired t-test, two-tailed: drug compared to vehicle. (h) Quantitative RT-PCR analysis of PDGFR β mRNA expression from isolated adipocytes treated with vehicle (DMSO) or rosiglitazone (5 μ M) for 4 hours. (i) Quantitative RT-PCR analysis of Angptl4 mRNA expression from FACS isolated AT-GFP⁺ cells from AT-control mice ($n = 6$) pretreated with cyclohexamide (10 μ g/ml) and subsequently treated with vehicle (DMSO) or rosiglitazone. # $P < 0.05$ unpaired t-test, two-tailed: drug treated compared to vehicle treated levels. (j) Schema of the PDGFR β promoter and putative PPRE site. ChIP-qPCR analysis for RXR occupancy on the putative PPRE of the PDGFR β promoter after treatment with vehicle (DMSO) or rosiglitazone (1 μ M). ** $P < 0.001$ unpaired t-test, two-tailed: RXR IP compared to IgG. Data are expressed as means \pm s.e.m.



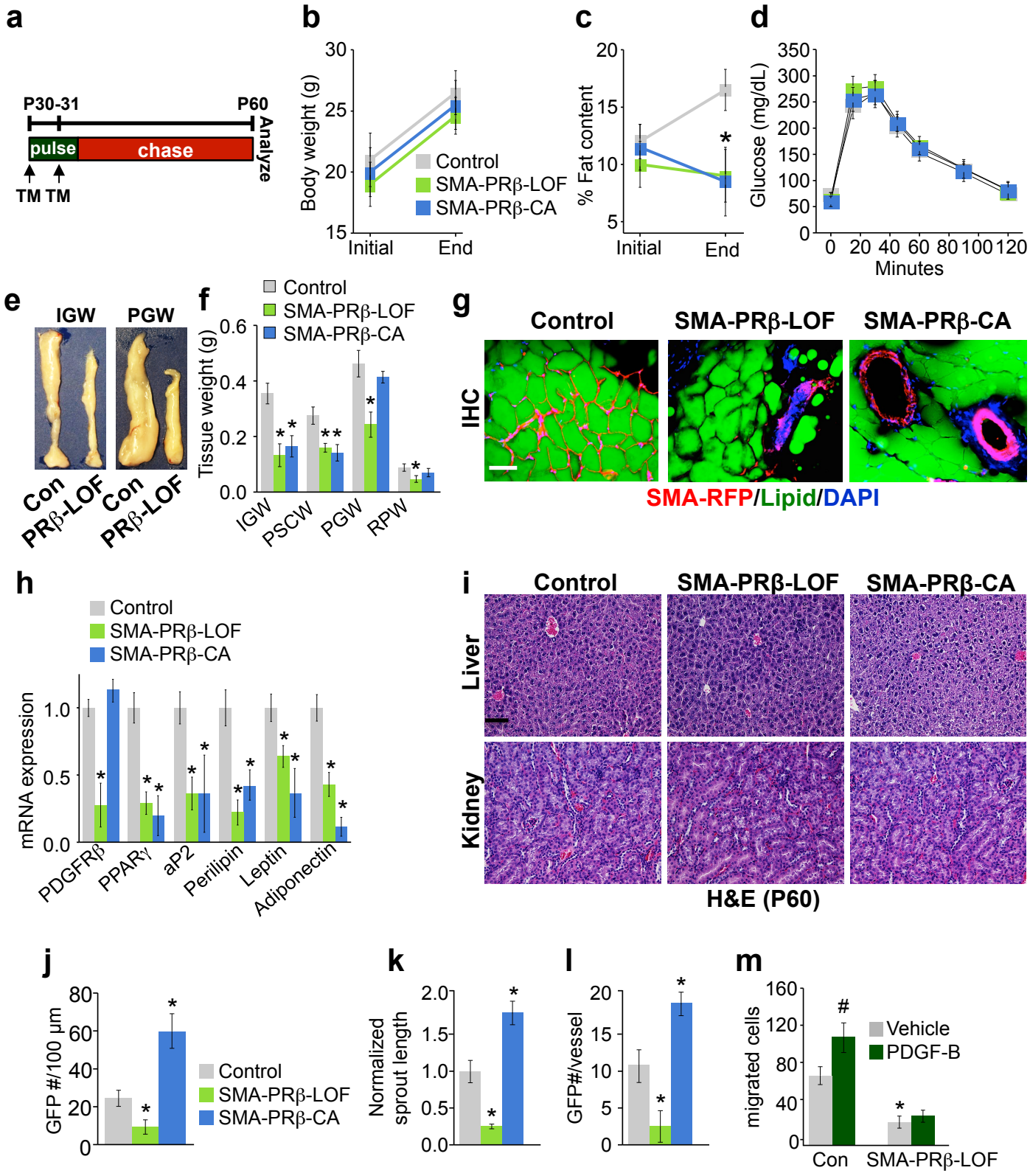
Supplementary Fig. 6 PDGFR β stimulates WAT niche expansion and APC-niche interaction

(a) Quantitative RT-PCR analysis of angiogenic markers and PDGFR β target genes from SV cells isolated from AT-Control, AT-PPAR γ -LOF and SMA-PPAR γ -LOF ($n = 6$) treated with vehicle (0.1% BSA) or PDGF-B (10 ng/ml) for 48 hours. * $P < 0.01$ treated compared to vehicle. (b,c) Representative images of SVPs isolated from AT-control mice ($n = 6$) treated with vehicle, PDGF-B (10 ng/ml) or SU16F (5 μ M) for 12 hours. APC-GFP fluorescence was imaged (b) and APC-GFP+ number was quantified per 100-micron SVP (c). Scale Bar 100 μ m. * $P < 0.01$ unpaired t-test, two-tailed: treated compared to vehicle. (d-f) Representative images of vascular sprouts from subcutaneous IGW explants from AT-control mice ($n = 8$). Explants were treated with vehicle, PDGF-B (10 ng/ml), SU16F (5 μ M), or PDGF-B (10 ng/ml) and SU16F (5 μ M). Vascular sprout length (d), branching (e) and AT-GFP sprout occupancy (f) were quantified. * $P < 0.01$ unpaired t-test, two-tailed: treated compared to vehicle. (g-i) Representative images of vascular sprouts from subcutaneous IGW explants of AT-control, AT-PPAR γ -LOF and SMA-PPAR γ -LOF mice ($n = 6$) treated with vehicle or PDGF-B (10 ng/ml). Vascular sprout length (g), branching (h), and sprouting (i) were quantified. * $P < 0.01$ unpaired t-test, two-tailed: treated compared to vehicle. ** $P < 0.01$ unpaired t-test, two-tailed: mutant compared to control. (j,k) Representative images of Boyden transwell migration chambers of FACS isolated APC-GFP+ cells from AT-GFP control mice ($n = 6$) pre-treated with vehicle or PDGF-B (10 ng/ml) for 48 hours prior to experimentation, migration was assessed 12 hours later (j). APC-GFP number was quantified (k). Scale Bar 100 μ m. * $P < 0.01$ unpaired t-test, two-tailed: treated compared to vehicle. (l-n) Representative image of modified Boyden transwell migration chambers of FACS isolated AT-GFP+ cells from AT-GFP control and AT-PPAR γ -LOF mice ($n = 6$) transfected with PDGFR β cDNA (l) and treated with vehicle or PDGF-B (10 ng/ml) for 12 hours (m). APC-GFP+ number was quantified (n). # $P < 0.01$ unpaired t-test, two-tailed: compared to AT-PPAR γ -LOF vector alone cells. * $P < 0.01$ unpaired t-test, two-tailed: treated compared to vehicle. Scale Bar 100 μ m. Data are expressed as means \pm s.e.m.



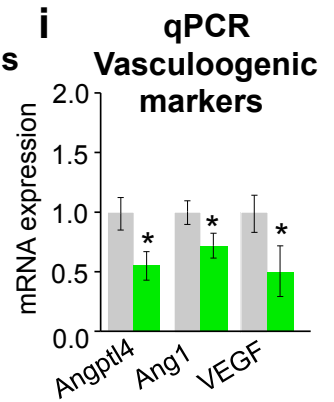
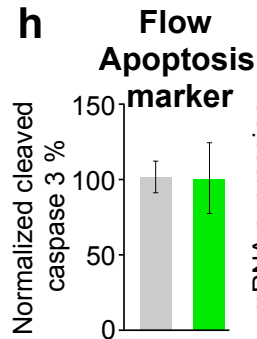
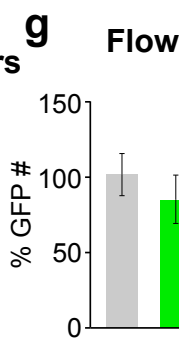
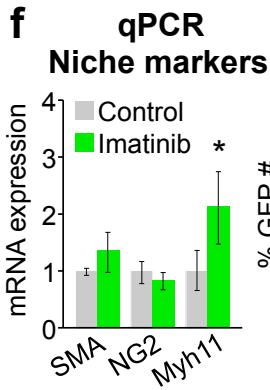
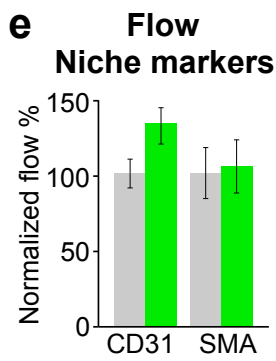
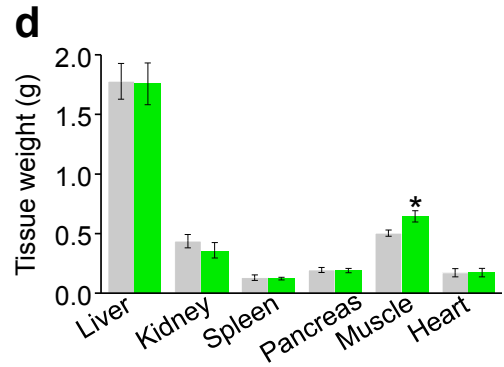
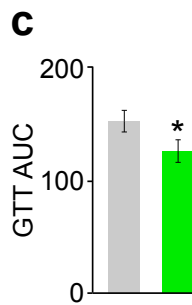
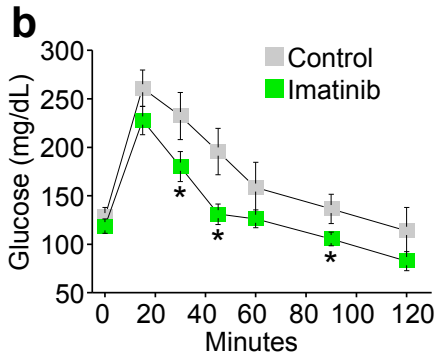
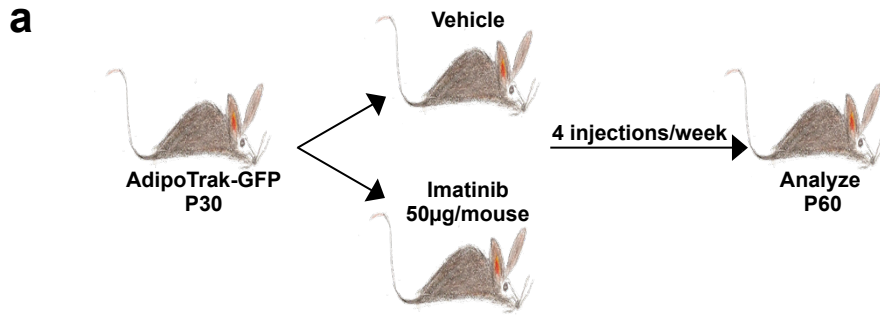
Supplementary Fig. 7 PDGFR β stimulates WAT niche expansion and APC-niche interaction

(a-c) Body weight (a), fat content (b), and lean mass (P60) (c) of AT-control, AdipoTrak PDGFR β loss (AT-PDGFR β -LOF) and constitutively active PDGFR β (AT-PDGFR β -CA) mice at denoted ages. Experiments were performed at least three times on 10 mice/group. (d) Representative images of H&E staining of subcutaneous IGW depots from mice described in (a) at P10. (e) Adipose tissue weights of mice described in (a) at P10. (f) Quantitative RT-PCR analysis of adipocyte markers from mice described in (a) at P10. (g) Representative photographs of subcutaneous IGW depots from mice described in (a) at P60. (h,j) Adipose tissue weight (h) and quantitative RT-PCR analysis of adipocyte markers (i) from mice described in (a) at P60. (j) Glucose tolerance test from mice described in (a) at P60. (k) Representative images of H&E staining of livers from mice described in (a) at P60. (l) Quantification of GFP number per 100-micron SVP. (m,n) Representative images of vascular sprouts from subcutaneous IGW explants from AT-control and AT-PDGFR β -LOF mice treated with vehicle or PDGF-B. AT-GFP+ occupancy per vessel capillary (m) and vessel sprouting (n) were quantified. (o) Representative images of modified Boyden transwell migration chambers of FACS isolated AT-control and AT-PDGFR β -LOF GFP+ cells pre-treated with PDGF-B for 48 hours. Migration was imaged 12 hours post plating. * $P < 0.05$ unpaired t-test, two-tailed: mutant compared to control. Scale Bar 100 μ m. Data are expressed as means \pm s.e.m.



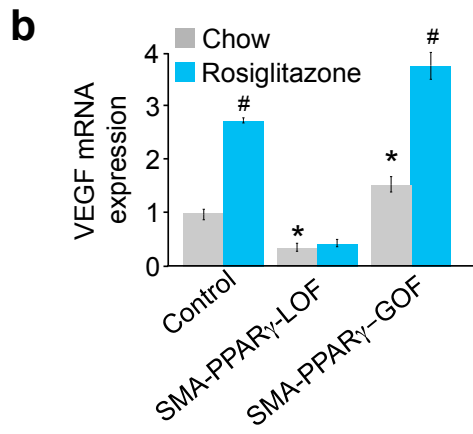
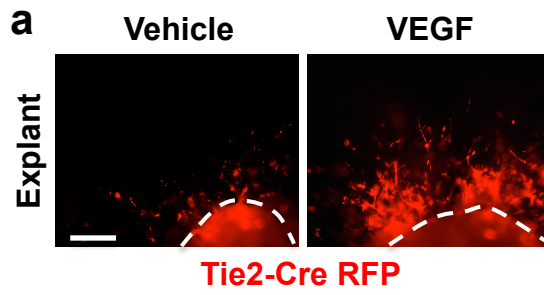
Supplementary Fig. 8 PDGFR β stimulates APC-niche retention

(a) Diagram of experimental paradigm. AT-GFP-SMA-control, AT-GFP-SMA-PDGFR β -LOF, and AT-GFP-SMA-PDGFR β -CA mice were administered one dose of tamoxifen for two consecutive days, mice were analyzed 30 days later. Experiments were performed at least three times on 10 mice/group. (b-f) Body weight (b), fat content (c), GTT (d), depot photograph (e), adipose tissue weight (f), SMA adipocyte fate mapping images, and quantitative-RT-PCR analysis of adipocyte markers were assessed from mice described in (a). (i) Representative images of H&E staining of liver and kidney from mice described in (a). (j) Quantification of AT-GFP number per 100-micron SVP. (k,l) Quantification of vascular sprout length (k) and APC-GFP occupancy (l) of subcutaneous IGW explants from mice described in (a). (m) Quantification of modified Boyden transwell migration chambers assays of FACS isolated AT-control and AT-PDGFR β -LOF GFP⁺ cells AT-SMA-control and AT-SMA-PDGFR β -LOF GFP⁺ cells pre-treated with PDGF-B for 48 hours prior to migration assessment. Migration was assessed 12 hours post plating. * $P < 0.05$ unpaired t-test, two-tailed: mutant compared to control. # $P < 0.05$ unpaired t-test, two-tailed: treated compared to vehicle. Scale Bar 100 μm . Data are expressed as means \pm s.e.m.



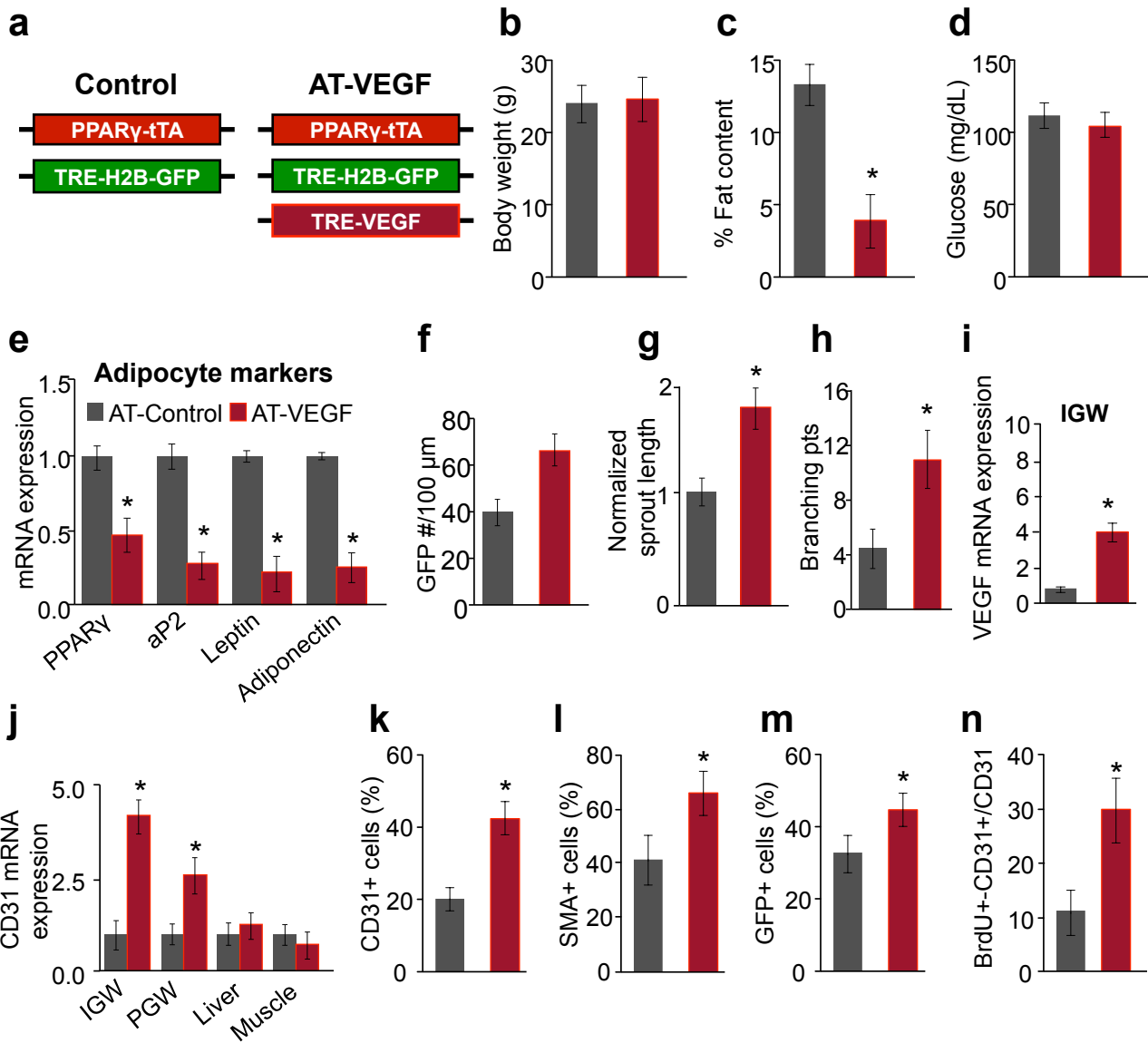
Supplementary Fig. 9 Pharmacologically blocking PDGFR β disrupts niche but improves glucose sensitivity

(a) Schema of experimental paradigm. AT-control male mice (P30) were administered vehicle (5%DMSO) or imatinib (50 ug/mouse) for four weeks. Experiments were performed three times on 8 mice/group. (b,c) Glucose tolerance test (b) and calculated area under the curve (c) of mice described in (a) at the end of treatment. (d) Tissue weights of denoted organs from mice described in (a). (e) The SV compartment was isolated from subcutaneous adipose depots from mice described (a). Cells were stained with antibodies against CD31 and SMA and were analyzed by flow cytometry for expression. (f) Quantitative RT-PCR analysis of niche markers from SV cells isolated from adipose depots from mice described in (a). (g) Quantification of APC-GFP number by FACS from the total SV compartment of subcutaneous adipose depots from mice described (a). (h) Quantification of cleaved caspase 3 by flow cytometry from the total SV compartment from isolated subcutaneous adipose depots from mice described (a). (i) Quantitative RT-PCR analysis of angiogenic markers from the total SV compartment from subcutaneous adipose depots from mice described (a). * $P < 0.01$ unpaired t-test, two-tailed: treated compared to vehicle. Data are expressed as means \pm s.e.m.



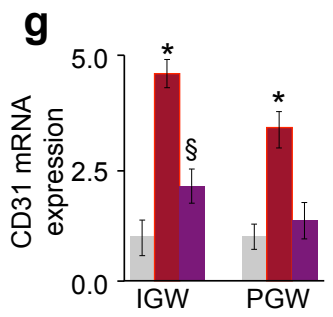
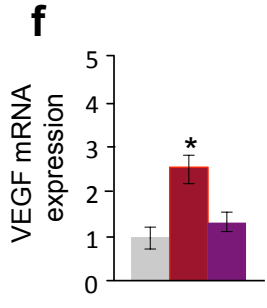
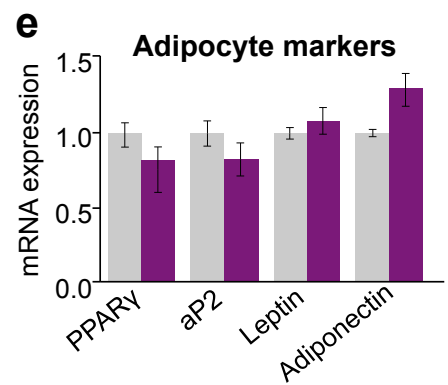
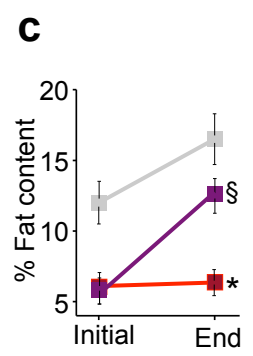
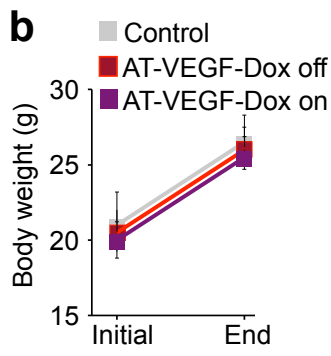
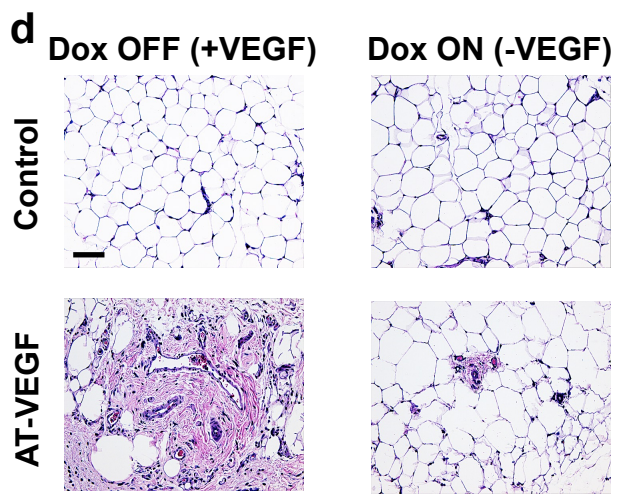
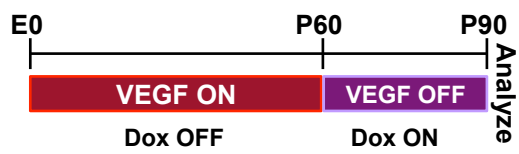
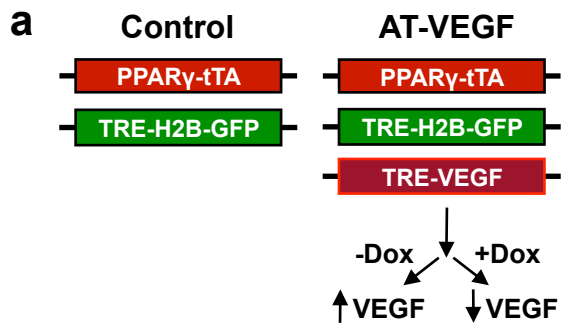
Supplementary Fig. 10 VEGF is a transcriptional target of PPAR γ in APCs

(a) Representative fluorescent images of vascular explants from subcutaneous IGW depots from *Tie2-Cre; Rosa26R^{RFP}* male mice treated with vehicle or VEGF (n = 3). (b) Quantitative RT-PCR analysis of PDGFR β mRNA expression from FACS isolated GFP+ cells from control, SMA-PPAR γ -LOF, and SMA-PPAR γ -GOF administered normal chow or rosiglitazone (0.0075% diet) for 7 days. * P <0.05 unpaired t-test, two-tailed: mutant compared control. # P <0.01 unpaired t-test, two-tailed: treated compared to vehicle. Scale Bar 100 μ m. Data are expressed as means \pm s.e.m.



Supplementary Fig. 11 VEGF stimulates nichegenesis but blocks fat formation

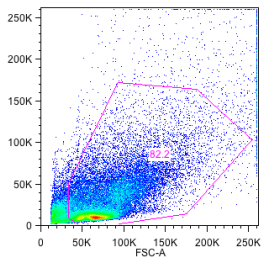
(a) Diagram of genetic strategy: AT-control and AT-VEGF ($PPAR\gamma^{+/tTA}; TRE-VEGF; TRE-H2B-GFP$). Experiments were performed three times on 10 mice/group. (b-e) Mice described in (a) were analyzed at three-months of age for body weight (b), fat content (c), random sera glucose (d), and quantitative RT-PCR analysis of adipocyte markers (e). (f) Quantification of APC-GFP number per 100-micron SVP. (g,h) Quantification of vascular spout length (g) and branching (h) from subcutaneous IGW depots from mice described in (a). (i,j) Quantitative RT-PCR analysis of VEGF (i), and CD31 (j) from denoted tissues from mice described in (a). (k-n) Total SV cells were isolated from subcutaneous IGW depots from mice described in (a). Cells were stained and examined for CD31 (k), SMA (l) and APC-GFP (m) positive cells or SV cells were examined for BrdU and CD31+ cells by flow cytometry (n). * $P < 0.01$ unpaired t-test, two-tailed: mutant compared to control. Data are expressed as means \pm s.e.m.



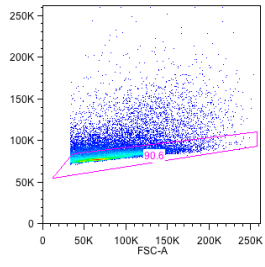
Supplementary Fig. 12 Suppressing VEGF expression in APCs restores niche function and promotes fat formation.

(a) Diagram of genetic strategy and experimental paradigm: AT-control and AT-VEGF were maintained off Dox until two months of age and then administered Dox for 30 days. Experiments were performed twice on 8 mice/group. (b,c) Body weight (b) and fat content (c) of mice described in (a) were assessed. (d) Representative images of H&E staining of IGW depots from mice described in (a). (e-g) Quantitative RT-PCR analysis of adipocyte markers (e), VEGF (f), and CD31 (g) mice described in (a). * $P < 0.001$ unpaired t-test, two-tailed: No Dox mutant compared to control mice. § $P < 0.05$ unpaired t-test, two-tailed: Dox suppressed mutant compared to control mice. Scale Bar 100 μm . Data are expressed as means \pm s.e.m.

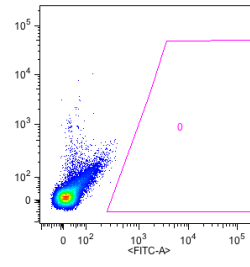
a Live cells



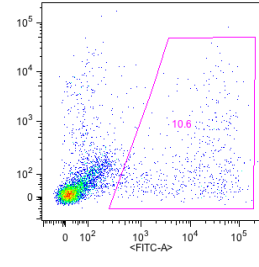
b Single cells



c Negative control

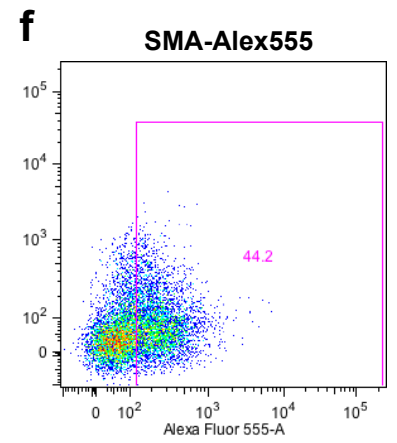
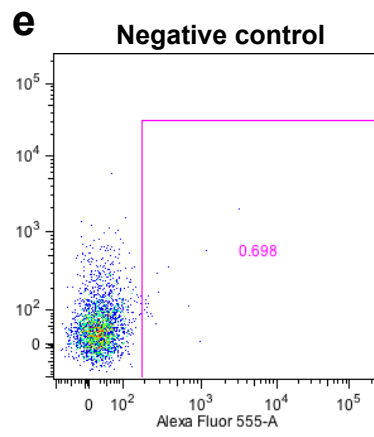
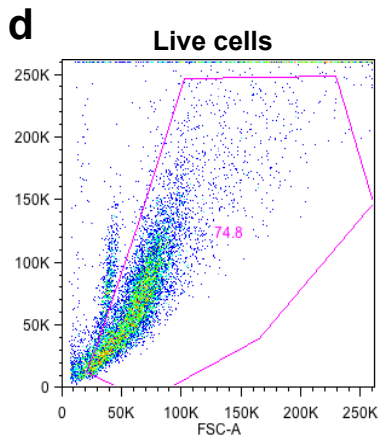
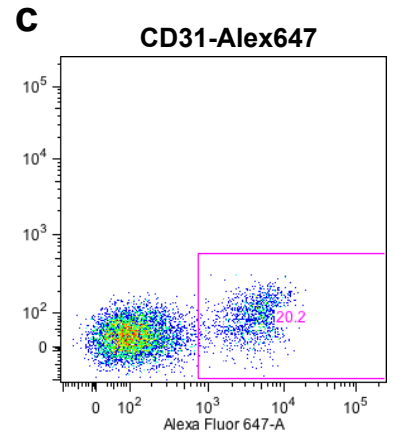
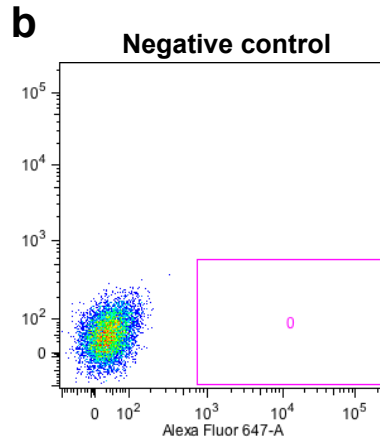
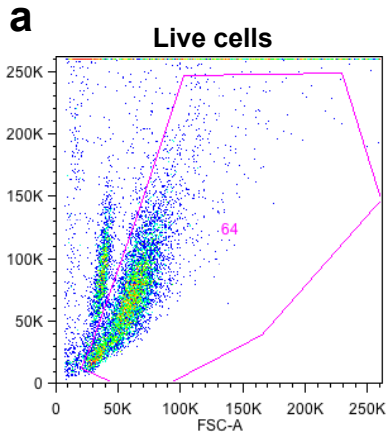


d GFP+



Supplementary Fig. 13 Gating strategy for the isolation of AT-GFP+ APCs by FACS

SV cells were first isolated from WAT depots of AT-GFP mice (n=3). **(a)** Live cells were selected by size on the basis of forward scatter (FSC) and side scatter (SSC). **(b)** Single cells were gated on both SSC and FSC width singlet's. **(c)** AT-GFP negative mice served as negative controls for gating. **(d)** Representative gating of GFP+ SVF cells isolated from AT-GFP control mice.



Supplementary Fig. 14 Gating strategy for flow analysis of CD31+ and SMA+ SVF cells

SV cells were first isolated from WAT depots of denoted mice. **(a)** live cells were selected by size on the basis of forward scatter (FSC) and side scatter (SSC). **(b)** Representative gating of donkey-anti-rat IgG Alexa647 (match to Cy5) antibodies stained cells as negative control. **(c)** Representative gating of CD31 stained positive cells. **(d)** live cells were selected by size on the basis of forward scatter (FSC) and side scatter (SSC). **(e)** Representative gating of donkey-anti-rabbit IgG Alexa555 (match to Cy3) antibodies stained cells as negative control. **(f)** Representative gating of SMA stained positive cells.

Supplementary Table 1. Primers for Real-Time PCR analysis

Genes	Forward	Reverse
<i>ACTA2</i>	GTCCCAGACATCAGGGAGTAA	TCGGATACTTCAGCGTCAGGA
<i>Adiponectin</i>	TGTTCTCTTAATCCTGCCCA	CCAACCTGCACAAGTTCCTT
<i>ADRP</i>	GACCTTGTGTCTCCGCTTAT	CAACCGCAATTTGTGGCTC
<i>Ang1</i>	CCAGGCCCGTTGTTCTTGAT	GGAAGGGAGACTTGCTCATTC
<i>Ang2</i>	AGAATAAGCAAGTCTCGCTTCC	TGAACCCTTTAGAGGCTCGGT
<i>Angptl4</i>	GTTTGCAGACTCAGCTCAAGC	CCAAGAGGTCTATCTGGCTCTG
<i>aP2</i>	AAGGTGAAGAGCATCATAACCCT	TCACGCCTTTCATAACACATTCC
<i>Axud1</i>	GTCTGTCCTCGGCTGTTGGAACC	CCACCTCAGCATCTCCAGCTTC
<i>CD18</i>	CAGGAATGCACCAAGTACAAAGT	CCTGGTCCAGTGAAGTTCAGC
<i>CD31</i>	ACGCTGGTGCTCTATGCAAG	TCAGTTGCTGCCATTTCATCA
<i>CD34</i>	AAGGCTGGGTGAAGACCCTTA	TGAATGGCCGTTTCTGGAAGT
<i>CD54</i>	CACAGTTCTCAAAGCACAGCG	GTGATGCTCAGGTATCCATCC
<i>CD106</i>	AGTTGGGGATTTCGGTTGTTCT	CCCCTCATTCTTACCACCC
<i>CD144</i>	CACTGCTTTGGGAGCCTTC	GGGGCAGCGATTTCATTTTTCT
<i>EGF</i>	AGCATCTCTCGGATTGACCCA	CCTGTCCCCTTAAGGAAAACCTCT
<i>FGF2</i>	GCGACCCACACGTCAAATA	TCCCTTGATAGACACAACCTCCTC
<i>KLF2</i>	CTCAGCGAGCCTATCTTGCC	CACGTTGTTTAGGTCCTCATCC
<i>Leptin</i>	GAGACCCCTGTGTGGTTC	CTGCGTGTGTGAAATGTCATTG
<i>Myh11</i>	AAGCTGCGGCTAGAGGTCA	CCCTCCCTTTGATGGCTGAG
<i>NG2</i> (<i>CSPG4</i>)	GGGCTGTGCTGTCTGTTGA	TGATTCCCTTCAGGTAAGGCA
<i>PDGF-B</i>	CATCCGCTCCTTTGATGATCTT	GTGCTCGGGTCATGTTCAAGT
<i>PDGFRβ</i>	AGGGGGCGTGATGACTAGG	TTCCAGGAGTGATACCAGCTT
<i>Perilipin</i>	GGGACCTGTGAGTGCTTCC	GTATTGAAGAGCCGGGATCTTTT
<i>PPARγ</i>	TCGCTGATGCACTGCCTATG	GAGAGGTCCACAGAGCTGATT
<i>Rn18s</i>	GTAACCCGTTGAACCCCAT	CCATCCAATCGGTAGTAGCG
<i>VEGF-A</i>	CTGCCGTCCGATTGAGACC	CCCCTCCTTGTACCACTGTC
<i>VEGFR2</i>	GCAGAAGATACTGTCACCACC	TTTGGCAAATACAACCCTTCAGA